Université de Mons
Faculté Polytechnique – Service de Mécanique Rationnelle, Dynamique et Vibrations
31, Bld Dolez - B-7000 MONS (Belgique)
065/37 42 15 – georges.kouroussis@umons.ac.be

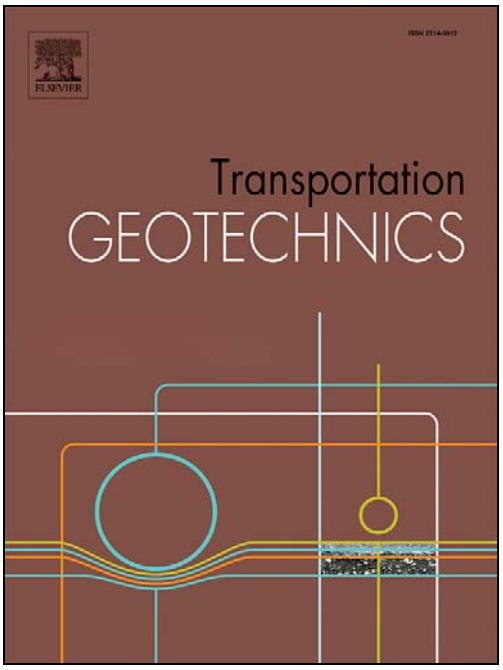

S. Qu, J. Yang, S. Zhu, W. Zhai, G. Kouroussis, Q. Zhang, Experimental study on ground vibration induced by double-line subway trains and road traffic, *Transportation Geotechnics*, 29, 100564, 2021.

Transportation Geotechnics 29 (2021) 100564

Contents lists available at ScienceDirect

Transportation Geotechnics

journal homepage: www.elsevier.com/locate/trgeo

Experimental study on ground vibration induced by double-line subway trains and road traffic

Shuai Qu [a], Jianjin Yang [a], Shengyang Zhu [a,*], Wanming Zhai [a], Georges Kouroussis [b], Qinglai Zhang [a]

[a] Train and Track Research Institute, State Key Laboratory of Traction Power, Southwest Jiaotong University, Chengdu, China
[b] Department of Theoretical Mechanics, Dynamics and Vibrations, Université de Mons, Belgium

ARTICLE INFO

Keywords:
Field experiment
Environmental vibration
Train-induced vibration
Ground vibration
Horizontal acceleration
Double-line subway

ABSTRACT

Rail transit and highway transportation have flourished in the process of urbanization by virtue of their respective advantages, facilitating people's travel but also producing harmful environmental vibrations. For an accurate analysis of source characteristics and propagation laws of train-induced vibrations, a field measurement was carried out in Shenzhen, China, where a double-line subway passes directly under the main urban road. The rail acceleration at the straight track and the point of fixed frog in the tunnel as well as ground vibrations caused by double-line subway and road traffic under different operating conditions were measured. A special attention was paid to the vibration response of each measurement point on the ground when the subway train and road vehicles passed through simultaneously. Measurement shows that horizontal acceleration cannot be ignored in the area close to the subway line, and vibration amplification phenomenon exists in the free field, due to the difference of the local geological conditions that leads to different vibration levels. Compared with the ground vibration caused by only the near-line train passage, when a near-line train passes the test section with a far-line train is about to arrive, the ground vibration intensifies in the frequency band of 50–63 Hz. When a far-line train passes the test section with a near-line train just left, the vibration level of each measuring point shows different degrees of reduction in various frequency bands, and reduction amount of horizontal acceleration in the frequency 10–16 Hz reaches 12 dB. Ground vibration aggravates significantly when the near-line train and bus pass simultaneously, the horizontal vibration is more sensitive to the superposition influence of road traffic. The measured data can not only guide the work of vibration environment assessment in the stage of subway design and planning but also can validate possible numerical models for predicting train-induced vibrations.

Introduction

Along with the advancement of urbanization, rail transit network is becoming increasingly large and complex. The resulting vibrations pose a considerable threat to people's daily production and life, the structural safety of buildings, and routine use of sensitive equipment, which is of increasing concern for transportation communities. In order to specifically design vibration reduction and isolation solutions, it is necessary to figure out the source characteristics and propagation laws of train-induced vibrations [6,11,22,29,31,35,36].

As for the vibration induced by subway trains, research focuses on the modeling of tunnel structure and surrounding soil. Some classical theoretical prediction models and methods have been proposed, such as PIP model [19], periodic structure method [8], 2.5-dimensional finite element method (2.5D FEM) [3], finite element-boundary element method (2.5D FEM-BEM) [28], finite element-infinite element method (2.5D FEM-IEM) [17], finite element- perfectly matched layers (2.5D FEM-PML) [27], finite element-method of fundamental solutions (2.5D FEM-MFS) [1]. In addition, the surrounding soil can be simplified into single-phase elastic half-space [14], layered half-space [18], saturated or unsaturated half-space model [13]. Further, the dynamic theory of vehicle-track system has also been introduced into the tunnel-soil dynamic system, and a series of accurate and efficient hybrid prediction models have been developed on this basis [2,4,39].

However, any theoretical analysis and numerical simulation cannot take all objective factors into consideration. The simplification of models and uncertainty of parameters will affect the calculation accuracy of prediction models [20,24]. The field vibration test is the most

* Corresponding author.
E-mail address: syzhu@swjtu.edu.cn (S. Zhu).

https://doi.org/10.1016/j.trgeo.2021.100564
Received 5 November 2020; Received in revised form 16 January 2021; Accepted 12 April 2021
Available online 16 April 2021

intuitive and accurate means to understand the vibration source excitation and the response of sensitive targets when the train passes, and it is also the only rigorous way that can check and evaluate analytical and numerical solutions. A large number of field experiments have been carried out in academic and engineering fields to provide accurate model parameters and test data to validate theoretical models [12,15,21,30,34,37,38,40,41].

The train-induced environmental vibration problems in the entry and exit section of subway stations often get less attention because of low operating speed. To facilitate the dispatching and maintenance of trains, turnouts are often laid in this area, which is called the three weak links of track along with curves and joints. When trains pass through these locations, large vibrations will be generated [4]. Further, the vibration problems caused by double-line subway trains are different from the vibration induced by only a single line has trains passing through. Therefore, it is necessary to measure and analyze this particular operating condition.

Despite the rapid development of rail transit in many countries and regions in the past decades, highway transportation also plays a leading role in urban transportation system due to huge advantages in route selection and private customization. In addition to polluting the air and causing traffic congestion, vehicles on the road will also cause noticeable ground vibration and noise problems, significantly affecting the vibration environment and sound environment in people's work and life. Hunaidi et al. [16], Crispino and D'apuzzo [7], and Watts and Krylov [32] conducted field experiments to analyze the ground vibration and building vibration induced by urban road traffic under different vehicle weights, running speeds, tire stiffnesses, and road smoothness. Watts [33] established a series of empirical rules based on experiments, using transfer functions to estimate ground vibration level caused by road traffic. Numerical methods have also been developed to simulate the effects of vehicle-hump interaction [10,23,26]. Compared with railway trains, the running speed and wheelbase of urban road vehicles are relatively small, and the induced ground vibration level under general conditions is limited [5,25]. However, for some special vehicles (such as heavy goods vehicles, fully loaded buses) or under particular circumstances (railway crossings, potholes, speed bumps and other areas, or pass simultaneously with railway trains), the environmental vibration caused by road traffic should not be ignored [10].

Reviewing the body of research on ground vibration induced by subway trains and road traffic, there are only a minimal number of studies analyzing the vibration effect of simultaneous operation [12]. Besides, there is also a lack of field tests on ground vibration caused by double-line subway trains. This paper relies on the Shenzhen Metro Line 11 to carry out field tests in the sections adjacent to the subway station. According to the different measuring point positions, the test can be divided into vibration source test in the tunnel and free field test. Special attention is paid to the ground vibration at the vertical and horizontal direction due to single-line train passing, double-line trains passing, and the rail transit operation superimposed by highway traffic. In order to have a better understanding of such a complex dynamic system, the in-tunnel and ground accelerations are analyzed in the time domain and frequency domain, respectively, and the test results can provide a reference for the research on environmental vibration caused by subway trains.

Field test site and experiment arrangement

The Shenzhen Metro Line 11 has a total length of 51.936 km, and it has the dual tasks of the airport express line and the Guangzhou-Shenzhen intercity rail line. There are many vibration-sensitive points along the route of Shenzhen Metro Line 11, including schools, hospitals, hotels, laboratories, government agencies, and residential buildings. The vibration and noise generated by train operation will not only adversely affect the equipment and passengers of the rail transit system but also affect the vibration environment along subway lines, where the routine use of nearby special-function equipment and rest of residents may be disturbed. The field test was conducted between Bihaiwan Station and Airport Station of Shenzhen Metro Line 11, and the test sections are adjacent to the subway station.

Due to geological sedimentation, the soil generally has prominent layered characteristics, which significantly impact the vibration and its propagation process in the soil. The original landform of the test section is a platform, which has been artificially filled. The exposed stratum includes artificially filled soil, strongly/slightly weathered rock. Groundwater mainly includes pores water and bedrock fissure water, which is generally ordinary in water abundance and permeability. According to geological borehole data, the soils with similar shear wave velocity are divided into one layer, in this way, the soil around the tunnel can be divided into three layers: the first layer is plain fill with an average thickness of 2 m; the second layer is mainly silty clay, the thickness of which is about 16–18 m, and the average thickness is 17 m; the third layer is mainly strongly weathered sandstone with a relatively large thickness. However, because the third layer is located below the tunnel, its nature has little impact on the transmission of vibration from the tunnel to the surface, so its thickness is no longer counted. The parameters of each layer of the soil are shown in Fig. 1.

The subway trains are in the form of 8 China Type-A subway vehicles (characteristic lengths and basic dynamic parameters of the vehicle are shown in Fig. 2 and Table 1, respectively), and the running speed of the trains in the test section is about 52 km/h. The wheelbase of the bus running in this area is 5.80 m, and the width of the car body is 2.50 m, as shown in Fig. 3. Axle load is 6500 kg at no load and increases to 11500 kg in the case of full load; the maximum speed of the bus running in this area is 69 km/h.

Measurement in the tunnel, located in the mining method tunnel at the subway entry and exit section, are selected at the straight track and the point of fixed frog, respectively, the test sections and track structure of the mining method tunnel are shown in Fig. 4. The measurement point at the straight track is 323.1 m away from the subway station, in comparison, another measurement point is 15.8 m away from the straight-track measurement point. The two test sections in the tunnel are all concrete sleeper monolithic track, and a standard rail with a mass of 60 kg per unit length is used. The turnout area adopts a single turnout of 60 kg/m rail (No. 9 straight pointed rail). The fastener system adopts DZIII fastener, with vertical stiffness of 40 kN/mm, horizontal stiffness of 30 kN/mm, and sleeper spacing of 0.6 m. The turnout fastener is a separate type III elastic strap fastener. The concrete's modulus of elasticity of the tunnel is $3.15 \times 10^4 N/mm^2$.

In order to obtain the vibration response of the rail and the ground induced by subway operation, a total of 7 sets of measurement points was arranged in the tunnel and the surface free field above the tunnel. As shown in Table 2, each set of measurement points contains two acceleration sensors. "T" and "F" stand for the abbreviations of "Tunnel" and "Free field" respectively, in which T1# is arranged on the straight track, and T2# is arranged at the point of fixed frog, recording the vertical and horizontal acceleration of rail. Measuring points F1#～F5# are located in the surface free field above the tunnel. They are evenly distributed along the normal direction of the tunnel centerline, with an interval of 20 m, each measuring point records measured vertical and horizontal (perpendicular to the track direction) vibration acceleration of ground. Due to the limitation of the test site, F1# is fixed in the plain fill by means of tooling, and F2#～F5# is fixed on the concrete pavement by plasticine, and the distribution of each measuring point on the ground is shown in Table 2. The tunnel corresponding to the ground test is a double-line composite tunnel, as shown in Fig. 5, 453 m from the subway station and the distance between centerlines of the two tunnels is 13.7 m, the design slope is 2/310, and the center of the tunnel is 14.65 m from the ground.

Several Dytran 3145A2 acceleration sensors (range: 1000 g, sensitivity: 0.6–0.8 $mV/m{\cdot}s^{-2}$) connected to a CRONOS-SL-2 dynamic data acquisition and analysis system (produced by German Integrated

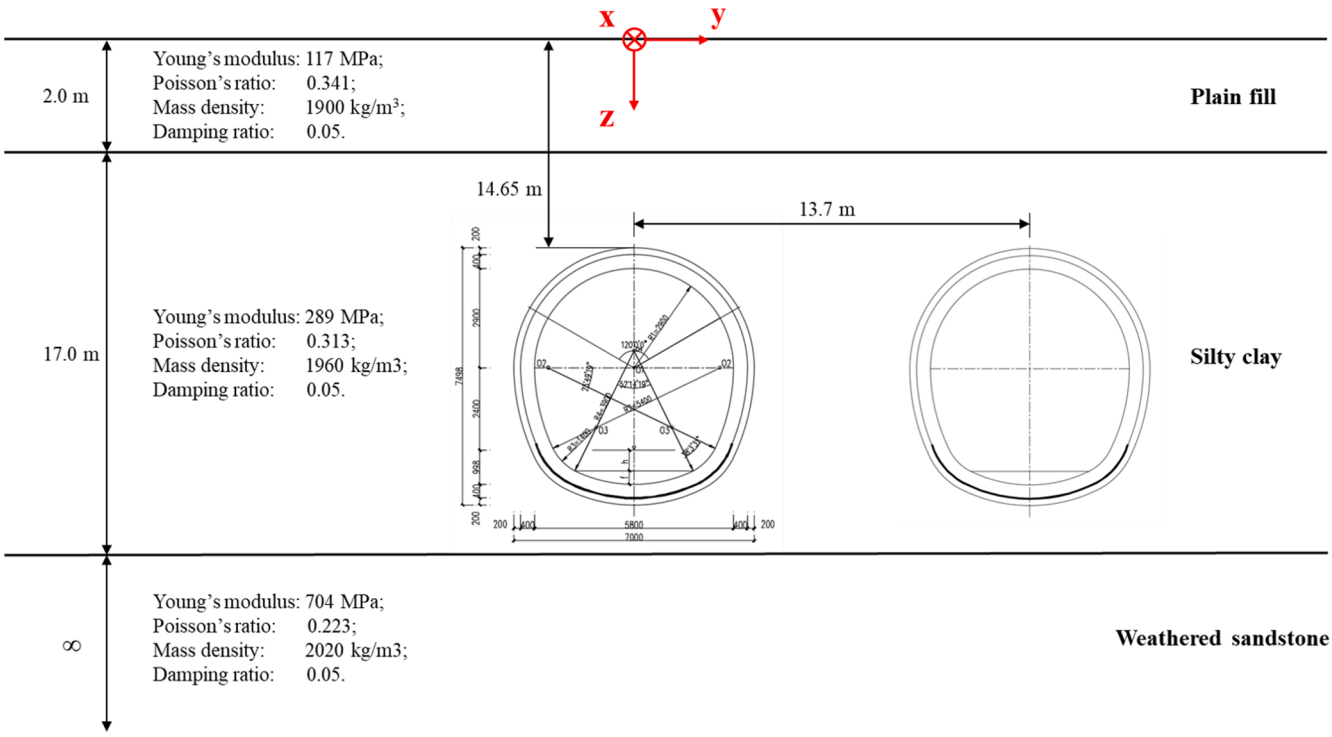

Fig. 1. Soil dynamic parameters.

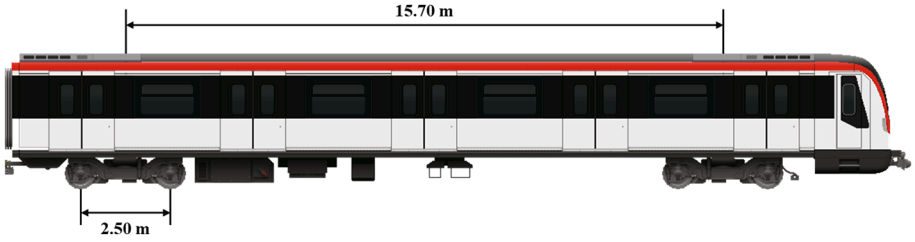

Fig. 2. The characteristic lengths of the subway train.

Table 1
Main parameters of subway vehicles.

Parameters	Vehicle	Units
Car body mass (M_c)	49.08	t
Bogie frame mass (M_t)	4.42	t
Wheelset mass (M_w)	1.68	t
Moment of inertia of car body (J_c)	1698.4	t·m^2
Moment of inertia of bogie frame (J_t)	4.90	t·m^2
Primary suspension stiffness (per axle box) (K_p)	1.27	MN/m
Primary suspension damping (per axle box) (C_p)	26.00	kNs/m
Secondary suspension stiffness (per bogie) (K_s)	0.27	MN/m
Secondary suspension damping (per bogie) (C_s)	16.2	kNs/m

Measurement & Control Company) are used for the rail test. The free-field test adopts the 991B vertical/horizontal vibration pickups from the Institute of Engineering Mechanics, China Earthquake Administration, with a range of 15 m/s^2 and resolution of 5×10^{-6} m/s^2. They are associated with INV3062A2, a 16-channel dynamic data acquisition and analysis system, from the China Orient Institute of Noise & Vibration. The whole set of test equipment is re-calibrated by the national authoritative testing department before use. The verification results show that this set of equipment is entirely suitable for micro-vibration detection, and the system performance is qualified.

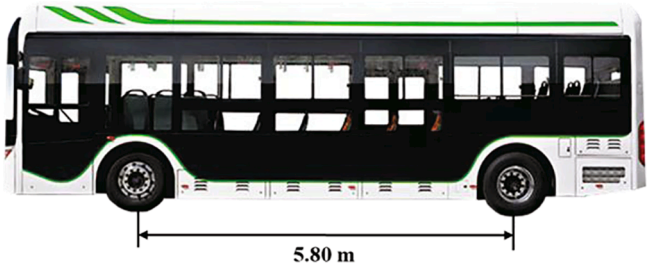

Fig. 3. The characteristic length of the bus.

Characteristic analysis of measured train-induced vibration

In this work, the measured vibration signals include the vibration response of the rail in the tunnel and the vibration response of the ground free field. Since the subway line consists of two parallel tunnels, the tunnel close to the ground measuring points is defined as "near-line tunnel", and the tunnel that is far from the ground measuring points is defined as "far-line tunnel". The corresponding test conditions are shown in Table 3.

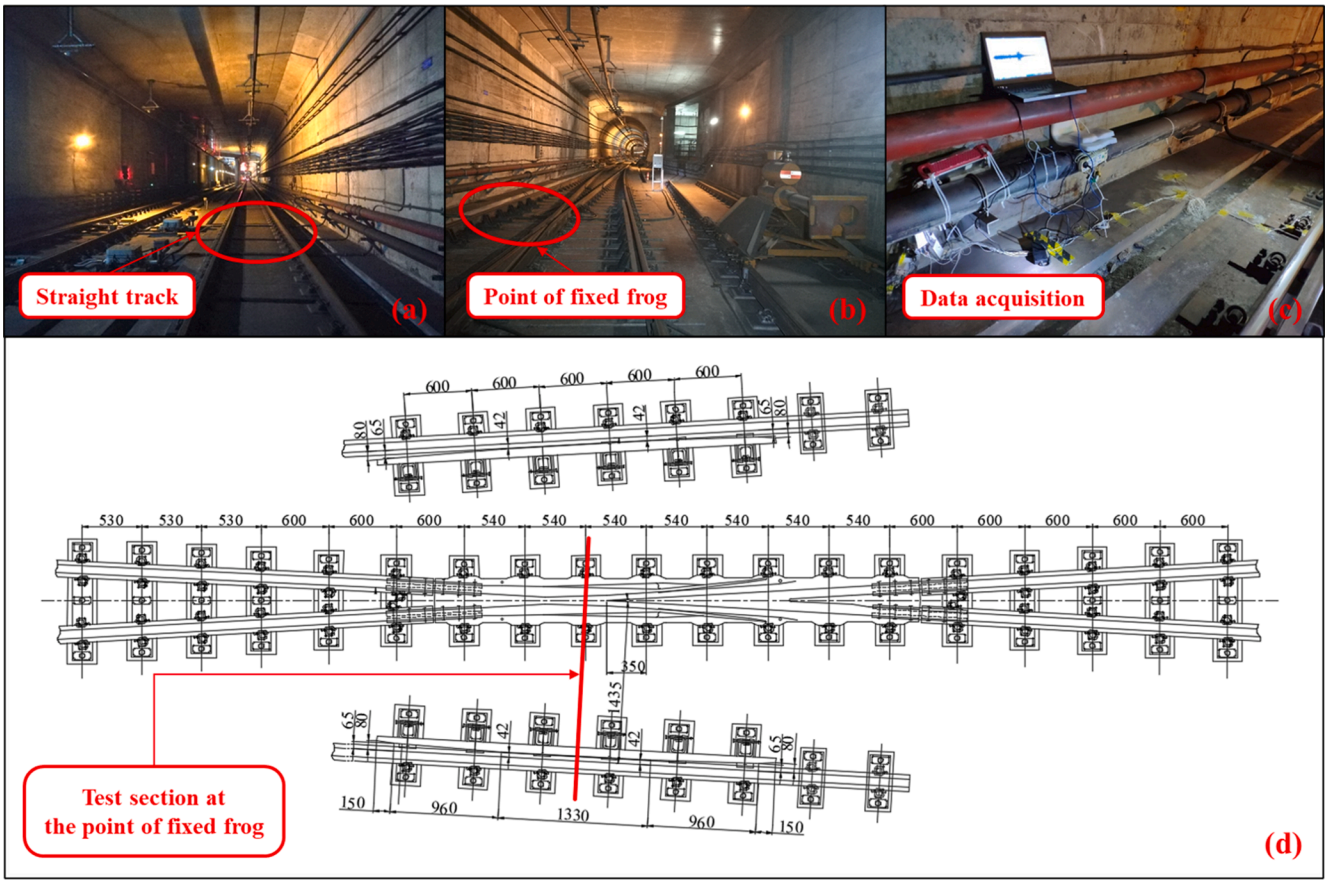

Fig. 4. Schematic diagram of test sites: (a) straight track; (b) point of fixed frog; (c) data acquisition system; (d) track structure at the point of fixed frog.

Table 2
Location and description of measuring points.

Location	Straight track	Point of fixed frog	Free field				
Measuring point number	T1#	T2#	F1#	F2#	F3#	F4#	F5#
Distance from subway centerline	–	–	20 m	40 m	60 m	80 m	100 m

Measurement in the subway tunnel

In order to accurately measure the vibration source characteristics of train-induced vibration, two sets of cross-sections were tested inside the tunnel: Section 1 (close to the subway station) located on the straight track, and Section 2 (away from the subway station) located at the point of fixed frog. Acceleration sensors are respectively arranged at the bottom and web of the rail of each section to record the vertical and horizontal acceleration of the rail. The vibration signals during the passage of the seven trains were collected, and the corresponding signal-to-noise ratio (SNR) is calculated as shown in Table 4, where "VRA" stands for vertical rail acceleration, and "HRA" stands for horizontal rail acceleration. It can be found that all the signal-to-noise ratios of the test signals are greater than 10 dB, indicating that the testing effect is good, and there is no need to modify the original data in the subsequent data analysis process.

The vibration response induced by train operation can be regarded as a stable random process that approximately follows the normal distribution. Table 5 lists the mean value of the vertical and horizontal acceleration of the rail induced by each train passing, and the variance of the vibration amplitude of the test signals is calculated in Table 6. It can be found that the mean value of each group of data is close to 0; namely, it follows a normal distribution with a mean of 0. Further, statistical analysis of variance of each group of data is conducted and calculate the coefficient of variation of the distribution of the dynamic response signal variance, as shown in Table 6. The values are all less than 15%, indicating there is no significant impact on the rail vibration acceleration due to the difference in operating conditions and the number of passengers during the seven trains passing, that is, the amplitude level of the vibration source is approximately the same. This also shows that in the subsequent vibration analysis of ground, the vibration response caused by different trains can be put together for comparative analysis.

In the collected rail vibration responses caused by seven train passages, the average peak value of the vertical and horizontal rail acceleration at the point of fixed frog are 127.619 m/s^2 and 74.115 m/s^2, which are respectively larger than those measured on the straight track, 113.116 m/s^2 and 69.763 m/s^2. The reason for this phenomenon is that the wheel-rail vibration excited by the turnout structure is more severe than the straight track, which leads to the difference in the amplitude of the vibration acceleration. Time history curves of vertical and horizontal rail acceleration are shown in Fig. 6. It can be seen that the vibration signal at the point of fixed frog can clearly distinguish the periodic vibration caused by bogies when the subway train passes. However, the same phenomenon is not apparent on the straight track. The reason is that the wheel-rail dynamic load excited by turnout structure will cause more significant sudden vibration, which will lead to an important amplitude change. When such excitation is transmitted to the rail, it appears as a periodic vibration effect. Due to the running speeds during the two test sections being relatively close, the measured vibration signals do not produce a considerable difference in amplitude.

To further understand the vibration characteristics of rail, the

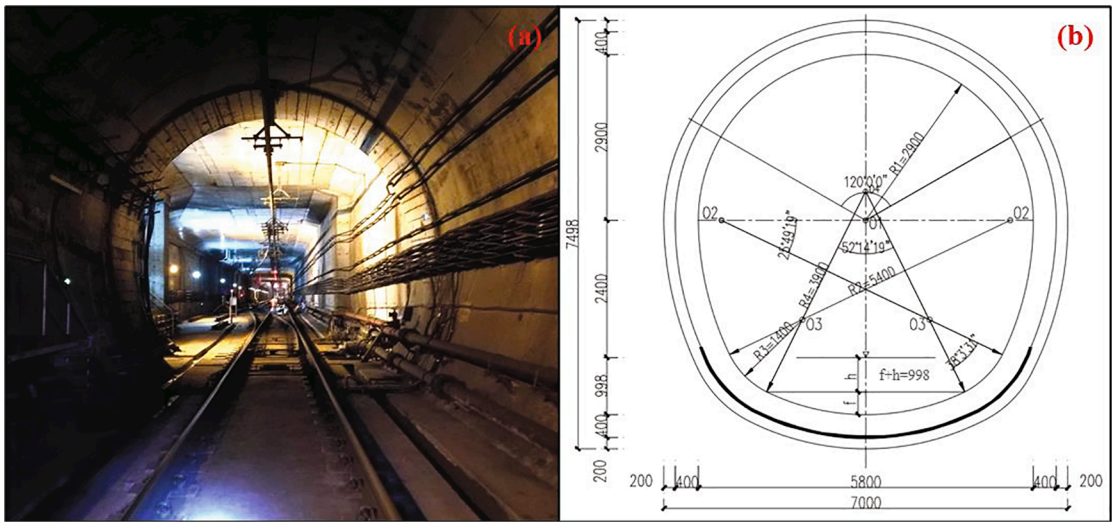

Fig. 5. Schematic diagram of the composite tunnel: (a) real scene; (b) tunnel size parameters.

Table 3
Free field test conditions.

Serial number	Condition description	Measuring point description
1	Near-line train passing.	A total of 5 sets of measuring points is arranged, with measuring points numbered F1#~F5#, each measuring point is arranged with an interval of 20 m along the normal direction of the subway line to test the vibration response at 20–100 m respectively.
2	Near-line train passing, far-line train is about to arrive.	
3	Far-line train passing, the near-line train just passed.	
4	Near-line train and bus pass simultaneously.	

Table 4
Signal-to-noise ratio of the measured signals.

Measurement number	SNR (dB)		Measurement number	SNR (dB)	
	VRA	HRA		VRA	HRA
Straight track −1#	43.846	37.435	Point of fixed frog −1#	42.314	42.914
Straight track −2#	42.875	36.143	Point of fixed frog −2#	43.022	44.529
Straight track −3#	43.923	37.189	Point of fixed frog −3#	42.236	43.483
Straight track −4#	43.791	37.047	Point of fixed frog −4#	42.448	43.598
Straight track −5#	44.472	37.561	Point of fixed frog −5#	42.516	42.605
Straight track −6#	44.511	37.887	Point of fixed frog −6#	42.779	42.920
Straight track −7#	43.637	37.355	Point of fixed frog −7#	42.436	43.596

measured vibration acceleration is converted to the frequency domain for analysis by discrete Fourier transform. Fig. 7 presents the frequency spectrum of the rail vibration acceleration measured at the two test sections. As respect for vertical rail acceleration, the main frequency components of the two sets of test data are concentrated in the frequency range of 50–80 Hz and 380–660 Hz. It is worth noting that there is a significant peak value at 1–8 Hz at the point of fixed frog, which covers the characteristic frequencies related to train speed (train speed between the measured sections is approximately 52 km/h) and bogie wheelbase (2.5 m). At the same time, there are multiple peaks at the straight track in the frequency range of 210–250 Hz, 280–330 Hz, 880–930 Hz and

Table 5
Mean value of the rail acceleration.

Test serial number	Mean (m/s^2)			
	Straight track		Point of fixed frog	
	Vertical	Horizontal	Vertical	Horizontal
1#	−0.00369	0.00367	−0.09276	−0.01640
2#	−0.00031	0.00125	−0.08791	−0.01892
3#	−0.00325	0.00472	−0.06225	−0.01025
4#	−0.00052	0.00676	−0.06288	−0.01144
5#	−0.00065	0.00488	−0.09020	−0.01646
6#	−0.00200	0.00121	−0.05894	−0.00954
7#	−0.00415	0.00489	−0.06300	−0.00385

Table 6
Variance of the rail acceleration.

Test serial number	Variance (m^2/s^4)			
	Straight track		Point of fixed frog	
	Vertical	Horizontal	Vertical	Horizontal
1#	332.90	91.96	125.91	84.17
2#	243.83	61.66	119.58	73.39
3#	275.29	70.62	110.60	75.77
4#	302.16	75.15	118.00	75.18
5#	327.86	87.68	138.14	84.98
6#	338.44	90.34	131.13	81.02
7#	306.06	77.63	120.17	75.08
Coefficient of variation (%)	11.28	14.18	7.41	6.08

higher frequency bands, which may be caused by short-wave irregularities on the rail surface. For the horizontal rail vibration acceleration, the main frequency components of the test signals at both sections concentrate in the frequency range of 45–115 Hz and 180–445 Hz. The difference of rail vibration lies mainly in prominent main frequency components above 1000 Hz at the straight track, which may be caused by more significant short-wave irregularities on the side of the rail on the straight track than near the turnout.

Ground vibration under different events

In this section, the ground free field vibrations induced by subway trains under different operating conditions are discussed in detail. The subway line locates directly under the highway, and there are five sets of acceleration sensors arranged at a distance of 20 m to 100 m from the

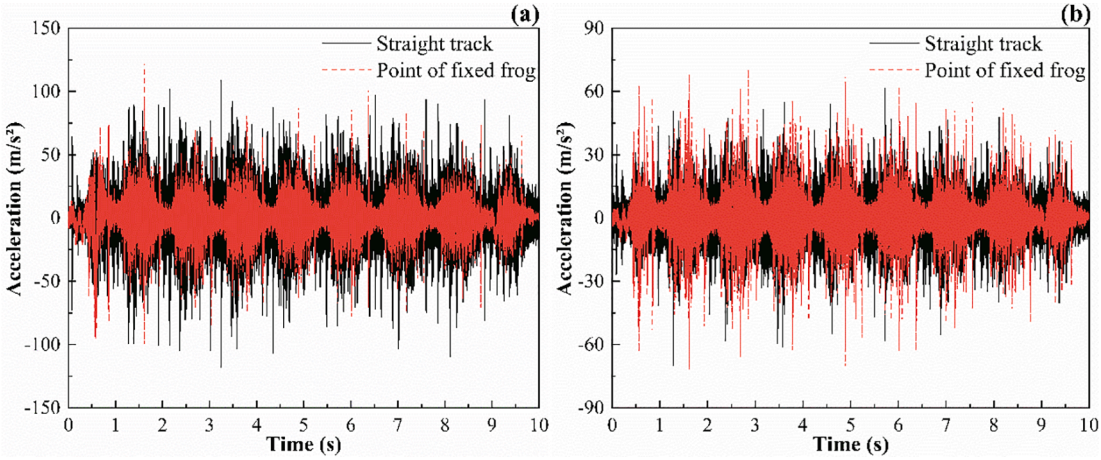

Fig. 6. Time-histories of rail vibration acceleration: (a) vertical acceleration; (b) horizontal acceleration.

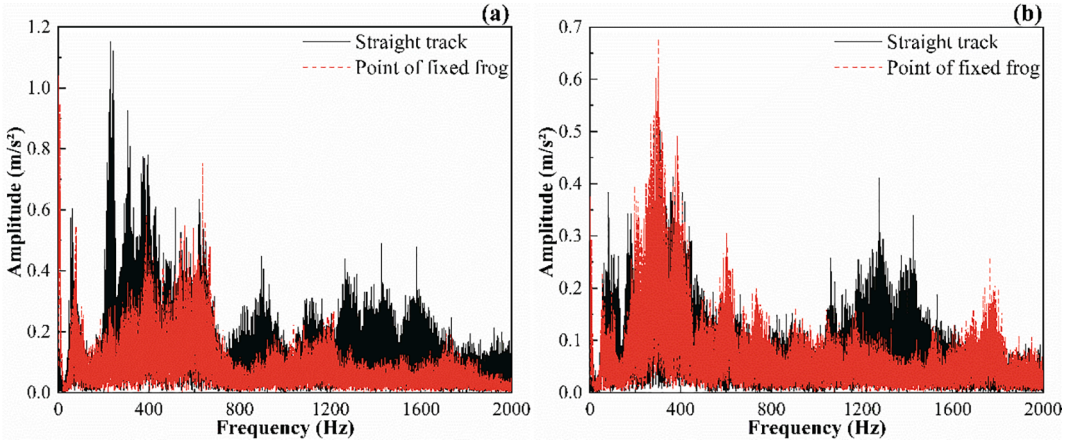

Fig. 7. Frequency spectra of rail vibration acceleration: (a) vertical acceleration; (b) horizontal acceleration.

subway centerline, with an interval of 20 m, to collect the vertical and horizontal (perpendicular to the track direction) acceleration of each measuring point, as shown in Fig. 8.

Ground vibration induced by single-line train passage

Although train-induced horizontal vibration is considered in some standards (such as ISO2631-2-1989), however, the regional environmental vibration evaluation and control standards formulated by various countries more recommend the vertical vibration index to evaluate the level of train-induced vibration, such as Chinese standard (GB 10070-201X), American standards (FRA 2005 and FTA 2006), British standard (BS6472-1-2008), German standard (DIN4150-2-1999, DIN 4150-3-1999), Dutch standard (SBR-Deel B 2006), Swedish standard (BVPO724.001), Norwegian standard (NS 8176E), Spanish Royal Decree (1367/2007). The field test found that the horizontal vibration in the area close to the subway line is also not negligible. Fig. 9 shows the typical time history curves of the measuring points on the ground when the near-line train passes. Compared with the vertical vibration,

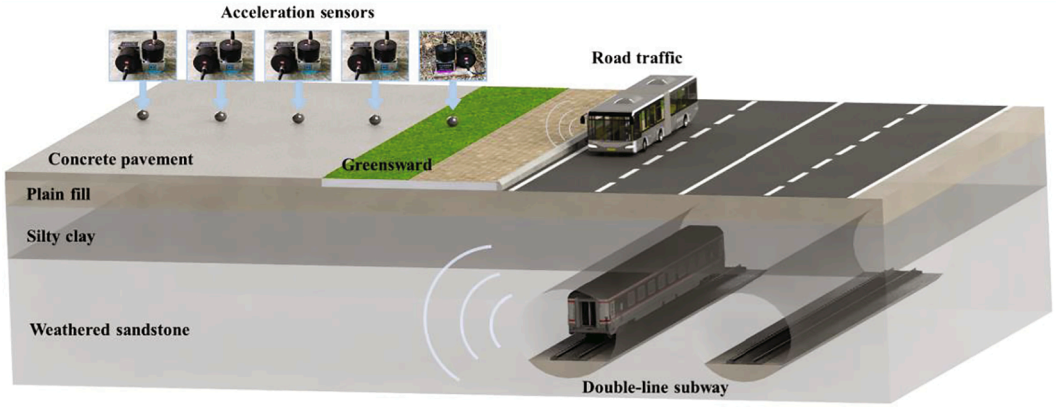

Fig. 8. Schematic diagram of test site.

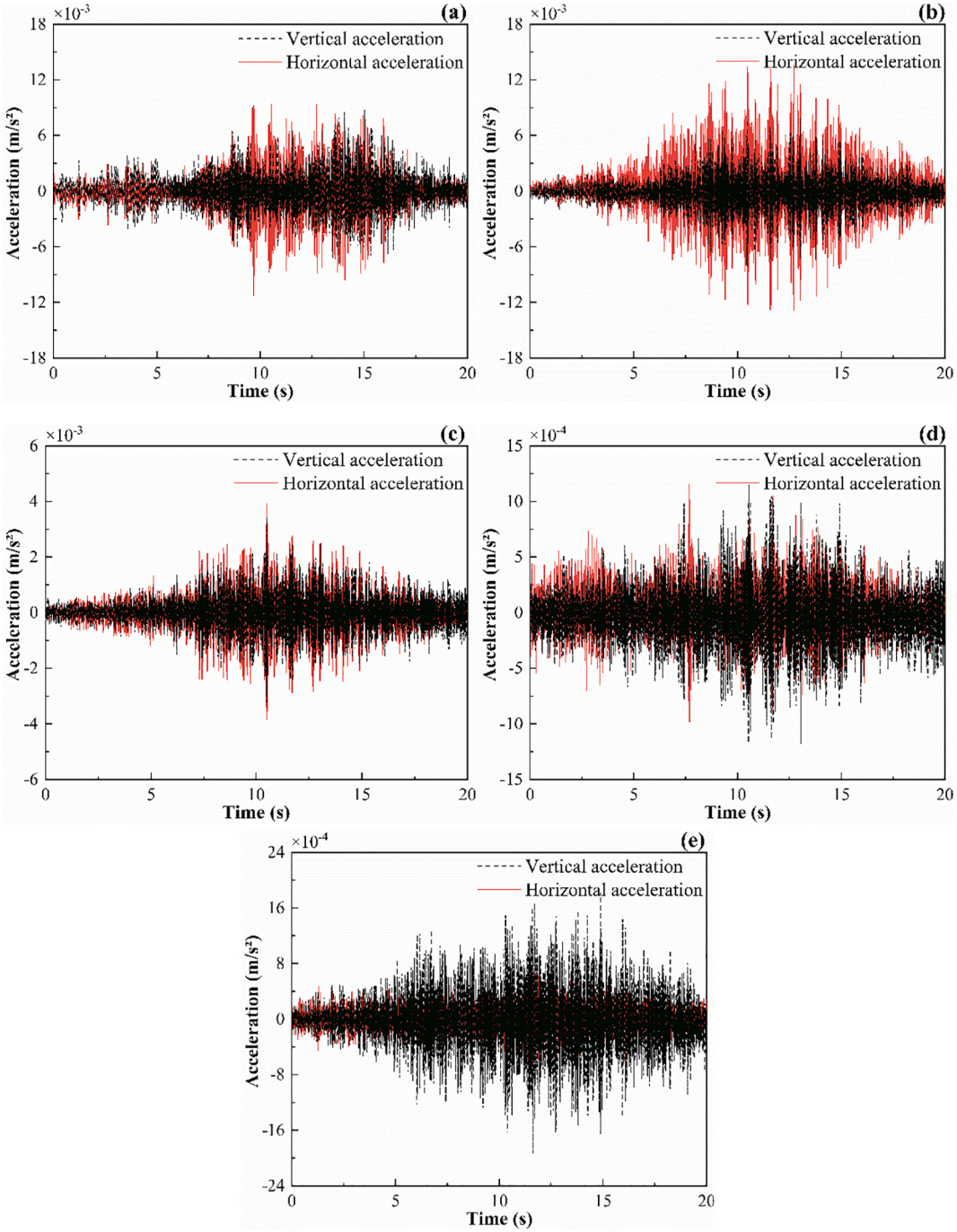

Fig. 9. Time-histories of ground acceleration induced by single-line train passage at different distance from subway centerline: (a) 20 m; (b) 40 m; (c) 60 m; (d) 80 m; (e) 100 m.

horizontal vibration caused by the passing of a train is apparent, especially at the position of 20 m and 40 m away from the subway centerline, the amplitude of the horizontal acceleration is significantly greater than that of the vertical direction, and it is gradually smaller than vertical vibration after 60 m. Besides, it is worth noting that the periodic effect caused by the passing of the train can still be observed at a distance of 100 m from the centerline of the subway; meanwhile, the horizontal vibration is attenuated up to the level close to the background noise.

The maximum vibration level (VL_{max}) is used as the evaluation index to analyze the variation law of ground vibration acceleration caused by train operation with distance, as shown in Fig. 10. It can be found that the vertical and lateral acceleration overall show a decreasing trend with the distance, mainly due to the radiation damping and material damping of the soil on the vibration wave. Besides, it can be observed that a vibration amplification phenomenon appears at 40 m and 100 m for the vertical direction, and at 40 m for the horizontal direction, similar phenomena have also been mentioned many times in previous studies [12,9].

At present, there is no widely accepted explanation for the causes of the vibration amplification zone. Some scholars believe that the repeated emission and refraction of elastic waves when propagating in the soft soil between the ground and the rock layer causes the vibration amplification. Some scholars believe that it is related to the underlying conditions and the buried depth of the tunnel. Others believe that this

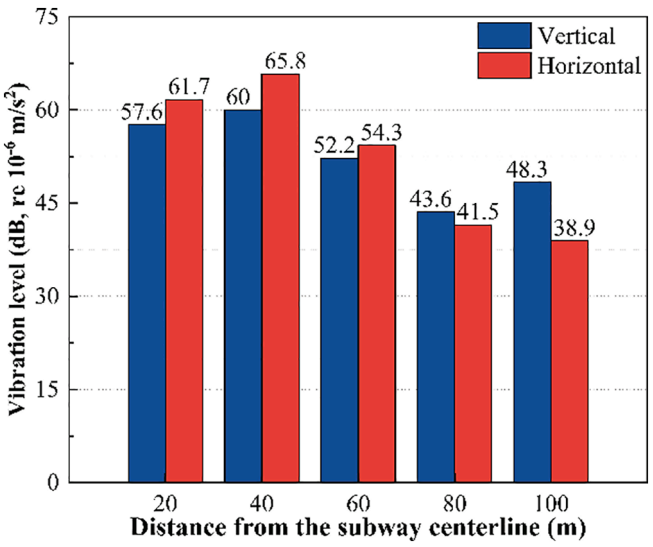

Fig. 10. VL_{max} varying with the distance from subway centerline induced by the passage of near-line train.

phenomenon is related to the peaks and troughs of the vibration wave in the propagation process, and the local geological conditions of the measuring points. In order to further explore the cause of the vibration amplification phenomenon in this test, the vibration response of each measuring point is converted into the frequency domain through Fourier transform for analysis, as shown in Fig. 11.

The black dotted line in Fig. 11 depicts the frequency components of the vertical acceleration. It can be found that at a position 20 m away from the centerline of the subway, the main frequency components of the vertical acceleration concentrate in 11–17 Hz, 28–30 Hz and 55–80 Hz, these frequency bands cover the characteristic frequencies related to train speed, sleeper spacing, and track irregularities. In detail, the train running speed between the test sections is about 52 km/h, the sleeper spacing is 0.6 m, and the vibration in the remaining frequency bands is mainly related to the short-wave irregularities of the rail surface ($L_{wavelength}$ = 0.18–0.26 m). As the distance increases, the vibration in the 11–17 Hz and 28–30 Hz frequency bands attenuates rapidly. The vibration in the frequency range of 48–68 Hz increases first and then attenuates, and reaches the maximum at the 40 m measuring point. The solid line in Fig. 11 represents the frequency components of the horizontal acceleration at different locations. The vibration attenuation law is the same as that of the vertical.

Particular attention should be paid to the main frequency components at the 40–100 m position (48–64 Hz), which has shifted from the 20 m position (46–50 Hz). This frequency band is also the main frequency band of vertical vibration. The explanation for this phenomenon is that in the actual test process, due to the limitation of the test site, the sensor at the position of 20 m is arranged on the plain fill through the tooling, while other sensors are arranged on the concrete pavement. The local geological conditions of the measuring points have been influenced by road hardening effect, which leads to the shift of main frequency components and vibration amplification.

Ground vibration induced by double-line trains successive passage

The vibration source intensity and characteristics of ground vibration induced by near-line train passage are analyzed in detail in the above sections. However, the environmental vibration problem will be more complicated when double-line subway trains pass successively. The reason is that when the near-line train passes the test section, the coming far-line train could have a certain effect on the propagation of ground vibration, as shown in Fig. 12(a). This effect also exists in the case that when the far-line train passes the test section, the near-line train has just left, as shown in Fig. 12(b). This kind of influence can lead to the amplification or reduction of ground vibration.

In order to distinguish the influence of nearby passing trains, the time-domain data of the near-line train passage (working condition as shown in Fig. 12(a)) and the far-line train passage (working condition as shown in Fig. 12(b)) are respectively calculated to obtain the vibration level in the one-third octave spectrum by Fourier transform. Fig. 13 shows the distribution of the vibration acceleration levels (VAL) of each measuring point in the vertical direction under three operating conditions, where the dotted line represents the vibration level when only the near-line train passes. According to VAL curve in Fig. 13(a), the main frequencies of ground vibration when the near-line train passes are 12.5 Hz, 31.5 Hz and 63 Hz, and the corresponding characteristic lengths are 1.12 m, 0.46 m and 0.23 m, respectively. With the increase of distance from the subway centerline, the vibration of the first two center frequencies attenuates rapidly; the vibration at 63 Hz attenuate slowly and gradually becomes the dominant component, indicating that the vibration wave in this frequency band is not easy to be attenuated by the soil in the process of propagation.

When the near-line train passes the test section, and the far-line train is about to arrive, it can be found from Fig. 13(a) that the vibration at 12.5 Hz and 31.5 Hz attenuates after superimposing the vibration effect of the far-line train, with the maximum attenuation degree of 10 dB at the measuring point of 20 m away from subway centerline. The VAL of other measuring points has also been reduced to a certain degree. However, the vibration level at the frequency of 63 Hz slightly increases after superimposing the influence of the far-line train. The maximum increment of VAL in the vertical direction is up to 10 dB at the measuring point of 80 m away from the subway centerline, and the increments of VAL of other measuring points all increase by 3 dB. This phenomenon indicates the vibration amplification effect under this operation condition only occurs around 63 Hz, with little effect on the vibration of other frequency bands, and even reducing the vibration in some frequency bands. This may be explained by the fact that the amplitudes of vibration waves excited by the two vibration sources decreases after superimposing due to the phase difference during the transmission process.

Different from the former condition, when the far-line train passes the test section and the near-line train just left, it can be found from Fig. 13(b) that except for the slight increase of VAL in the vertical direction at the position of 80 m away from subway centerline, the vibration levels of remaining measurement points in almost all frequency bands are smaller than that caused by only the near-line train passage. This phenomenon may be attributed to the fact that the distance between the vibration source and measurement points plays a more prominent role in the transmission of vibration waves.

Similar to the vertical vibration acceleration level, Fig. 14 shows the distribution of the horizontal vibration acceleration level in the one-third octave spectrum of each measuring point. When only the near-line train passes, the VAL of ground in the horizontal direction at the measuring point of 20 m mainly concentrates at 10–16 Hz and 31.5–63 Hz, the corresponding characteristic lengths of which are 1.44–0.90 m, 0.46–0.23 m, respectively. The horizontal vibration in the subsequent measurement points decays rapidly within the frequency of 10–16 Hz, and the VAL in the horizontal direction mainly concentrates in the range of 40–80 Hz, with corresponding characteristic length ranging from 0.36 to 0.18 m. Like the above analysis, the potential reason for this phenomenon is that the pavement hardening phenomenon exists in the installation foundation of subsequent measuring points compared to the 20 m one, which results in the change of the main frequency components of vibration.

When the near-line train passes the test section, and the far-line train is about to arrive, it can be seen from Fig. 14(a) that the horizontal vibration acceleration level of each measuring point in the 10–16 Hz reduces significantly, and the maximum attenuation degree of the vibration level reaches 15 dB at the measuring point of 20 m. After superimposing the vibration effects of the far-line train, it can be found

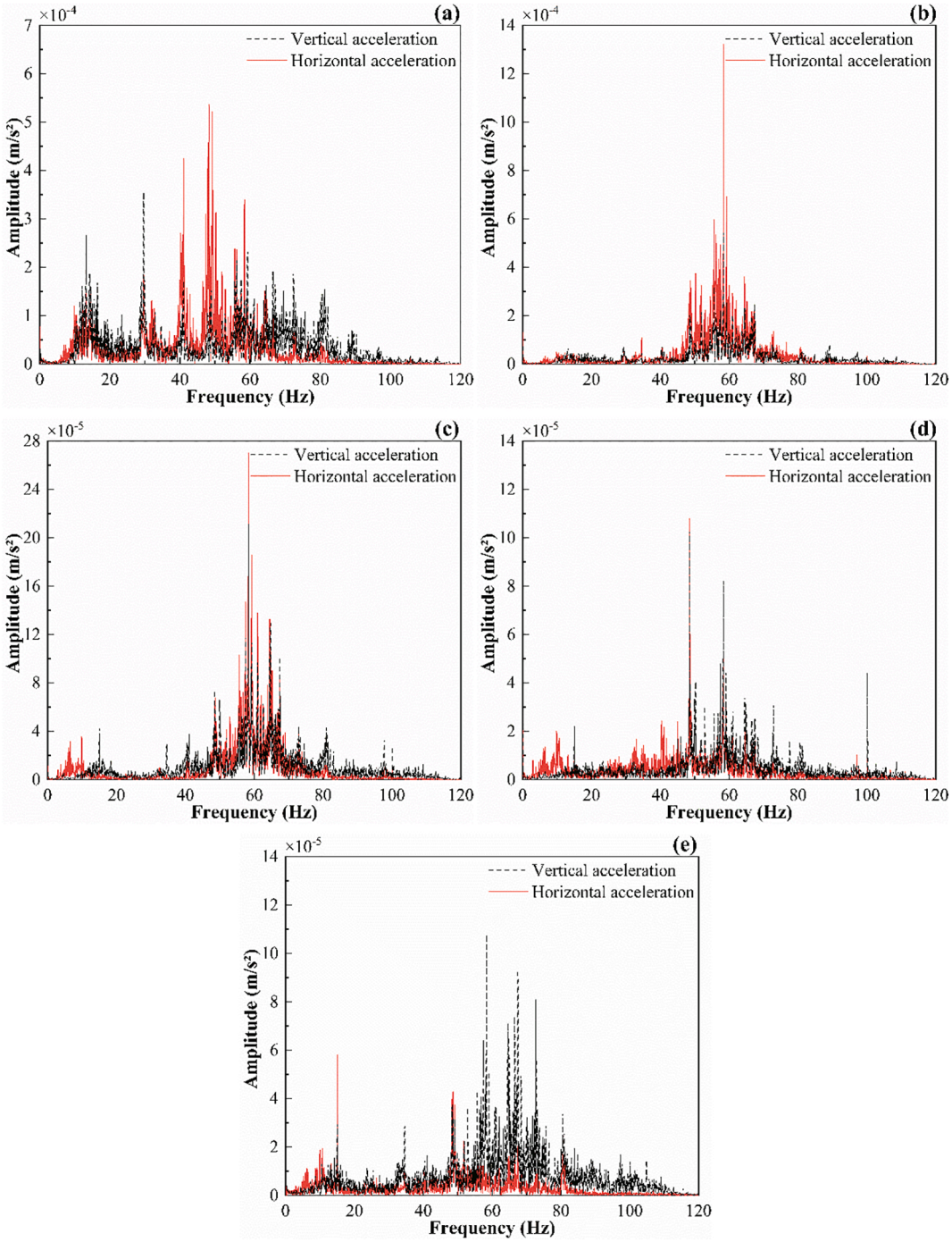

Fig. 11. Frequency spectra of ground acceleration induced by single-line train passage at different distance from subway centerline: (a) 20 m; (b) 40 m; (c) 60 m; (d) 80 m; (e) 100 m.

that the vibration level of each measuring point in the 50–63 Hz frequency band all increases, with a maximum increase of 8 dB at the position of 80 m.

When the far-line train passes the test section, and the near-line train just left, it can be seen from Fig. 14(b) that the main frequency components of the horizontal vibration acceleration levels are the same compared to the aforementioned test condition. The difference lies in the horizontal vibration level of each measuring point decreases in various frequency bands to different degrees after superimposing the influence of the near-line train vibration. The vibration reductions all reach 12 dB in the 10–16 Hz frequency band at the measuring points of 20 m, 60 m, and 80 m away from the subway centerline. Therefore, it can be concluded that the horizontal vibration level induced by the far-line train superimposed with the effect of a nearby near-line train is lower than that when only the near-line train passes.

Ground vibration induced by simultaneous passage of subway train and road traffic

The vibration characteristics of the ground under single-line train and double-line trains passage are analyzed in detail in the above sections. However, when subway trains and road traffic pass simultaneously, changes will happen to the vibration law. Some scholars have used traffic lights to control traffic flow to study the environmental vibration caused by road traffic and subway operation [12]. However, due

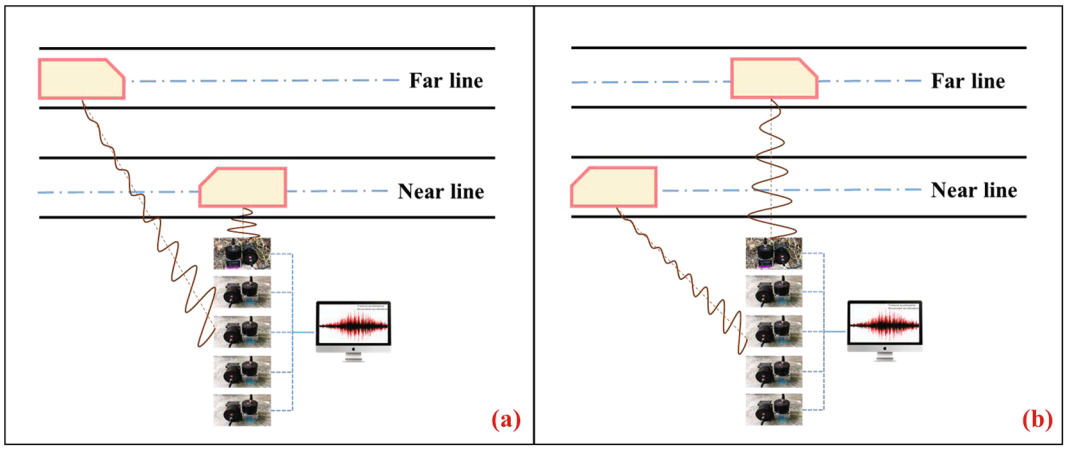

Fig. 12. Schematic diagram of test conditions: (a) when the near-line train passes the test section, the far-line train is about to arrive; (b) when the far-line train passes the test section, the near-line train has just left.

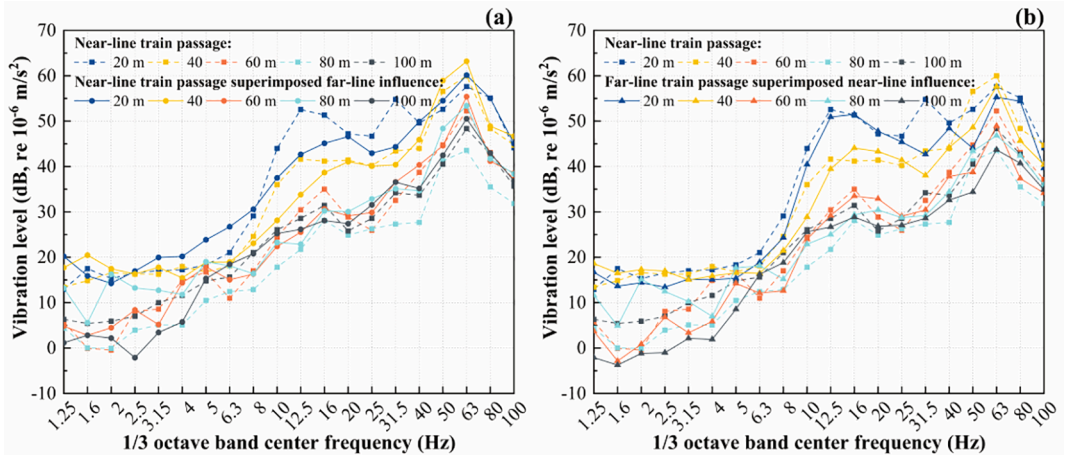

Fig. 13. The vertical vibration acceleration level in the one-third octave spectrum: (a) the near-line train passes, and the far-line train is about to arrive; (b) the far-line train passes, and the near-line train has just left.

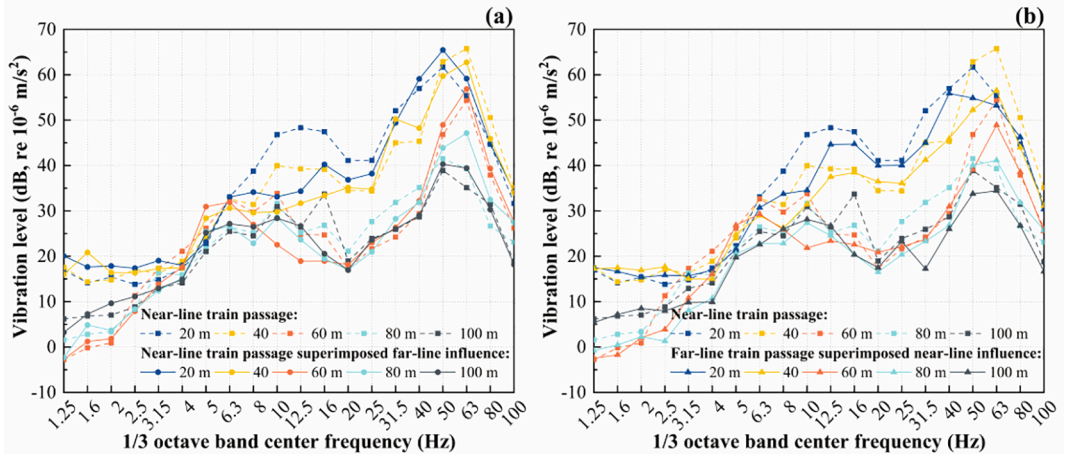

Fig. 14. The horizontal vibration acceleration level in the one-third octave spectrum: (a) the near-line train passes, and the far-line train is about to arrive; (b) the far-line train passes, and the near-line train has just left.

to the limitation of test requirements, the vibration transmission law induced by the simultaneous passage of subway train and road traffic has not been studied in detail. The work in this section detects that there is just one bus passing on the nearby road when the near-line train passes. Fig. 12 shows the vibration response of each measuring point when the near-line train and the ground bus pass the test section simultaneously, where the blue dotted line selects the time (9.5–11.2 s) bus is passing through. From the comparative analysis of Fig. 9(a) and

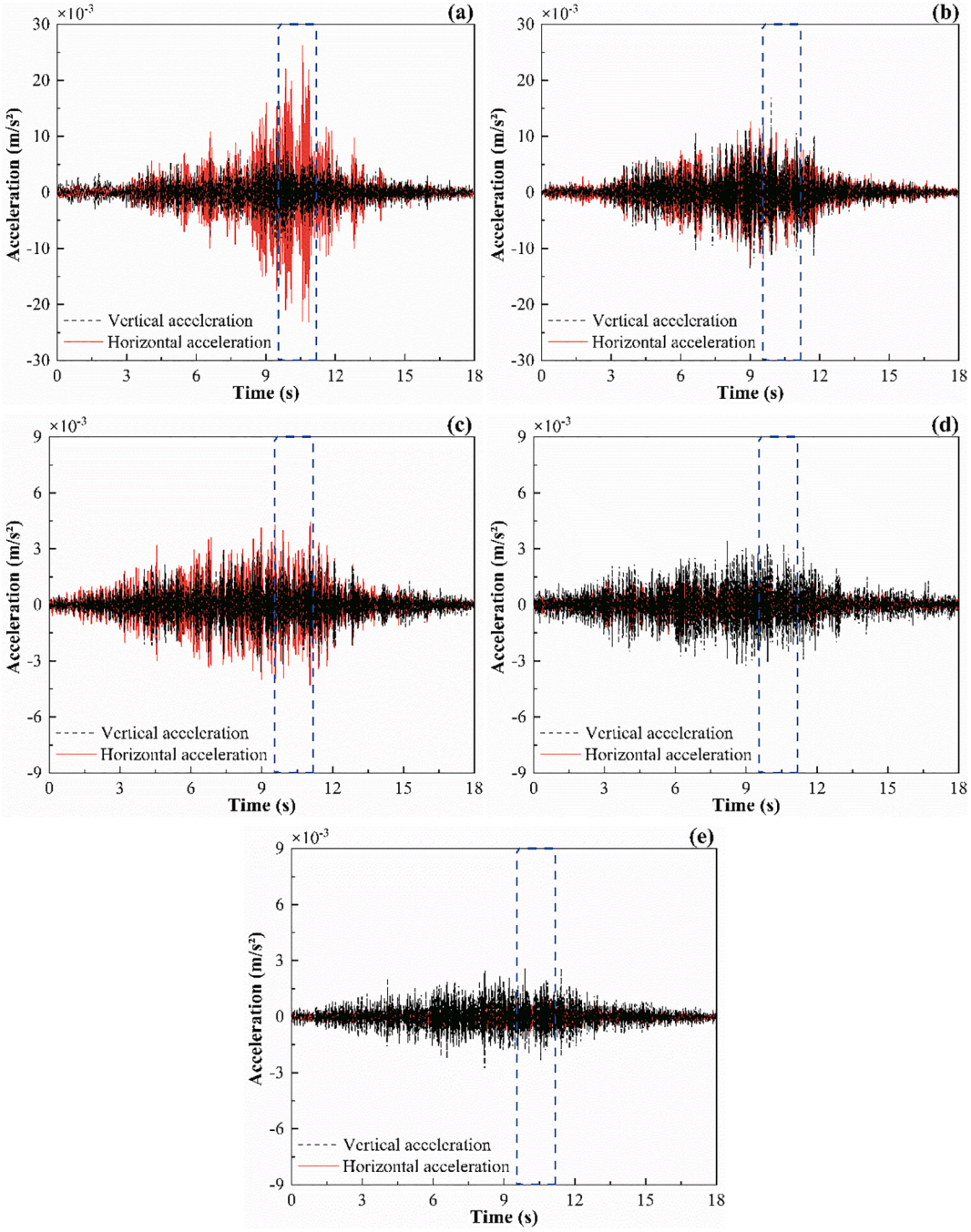

Fig. 15. Time-histories of ground acceleration induced by the simultaneous passage of subway train and road traffic at different distance from subway centerline: (a) 20 m; (b) 40 m; (c) 60 m; (d) 80 m; (e) 100 m.

Fig. 15(a), it can be found that the vibration acceleration level at a measuring point 20 m from the subway centerline significantly increases after the impact of bus vibration is superimposed. The maximum vertical acceleration on the ground is 1.27×10^{-2} m/s^2; the increase is up to 47.16% compared with when only near-line train passes. The peak value of horizontal vibration acceleration is 2.62×10^{-2} m/s^2, the increase is up to 181.80%. This indicates that when the subway train and road traffic pass at the same time, the ground vibration in the adjacent area will increase significantly, and the horizontal ground acceleration is more sensitive to road traffic.

At the subsequent measurement points, as the distance from the centerline increases, the ground vibration acceleration decays rapidly, and the horizontal acceleration attenuates more severely. From the measuring point at 40 m, horizontal vibration attenuates to a level close to when only the near-line train passes. At this position, the peak vertical acceleration is 1.72×10^{-2} m/s^2, with an increase of 114.86%. Subsequently, the vertical vibration restores to the same level as when only the near-line train passes. This phenomenon shows that the ground vibration caused by road traffic decays rapidly with the increase of distance, and horizontal vibration decays faster than the vertical vibration.

Similarly, the vibration data of each measurement point in the time domain is converted into one-third octave spectrum through Fourier transform to analyze the frequency characteristics of the ground vibration when the subway and bus pass simultaneously, as shown in Fig. 16. According to the previous analysis, when only near-line trains pass by, the main frequencies of vertical ground vibration are 12.5 Hz, 31.5 Hz,

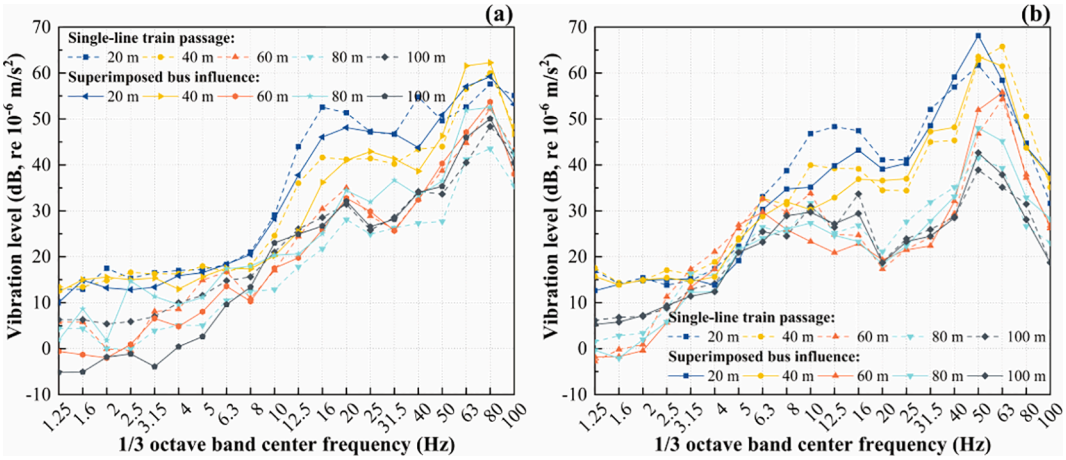

Fig. 16. The vibration levels in the one-third octave spectrum when the subway and bus pass simultaneously: (a) vertical vibration; (b) horizontal vibration.

and 63 Hz, and the corresponding characteristic lengths are 1.12 m, 0.46 m and 0.23 m, respectively. The dominant frequencies of horizontal vibration concentrate at 10–16 Hz and 31.5–63 Hz, and the corresponding characteristic lengths are 1.44–0.90 m and 0.46–0.23 m, respectively. After superimposing the vibration impact of road traffic, the vertical and horizontal vibration levels increase significantly at 20 m, and the horizontal vibration amplifies more severely. As the distance from the centerline increases, the ground vibration attenuates rapidly, and the vertical vibration attenuates more slowly than the horizontal vibration.

Based on the vibration characteristics of road traffic, the two measurement points (20 m, 40 m) close to the centerline are mainly analyzed. It can be seen from Fig. 16(a) that the vibration peaks of the vertical ground vibration at the center frequency of 12.5 Hz and 31.5 Hz both reduce at the 20 m measurement point. The vibration level of 12.5 Hz reduces by 6.4 dB, and the vibration level of 31.5 Hz reduces by 11.1 dB. However, vibration amplification appears in the 63–80 Hz frequency band, increasing by 4.8 dB at most. Similar vibration rules also appeared at the measuring point at 40 m, but the changes in vibration levels are slightly smaller than that at 20 m.

The primary frequencies of horizontal vibration concentrate at 10–16 Hz and 31.5–63 Hz, as shown in Fig. 16(b), the vibration around 10–16 Hz significantly reduced after superimposing the influence of road traffic. The maximum vibration reduction occurs at the 10 Hz frequency by 11.7 dB at the measuring point of 20 m, and the vibration reduction at the measuring point of 40 m also reaches 9.5 dB. Meanwhile, it can be observed that when the near-line train and the bus pass simultaneously, the ground vibration in the 40–80 Hz frequency band amplified, and the maximum vibration amplification reaches 6.6 dB at the center frequency of 50 Hz, the law of which is also the same as the above analysis.

Through the analysis of the frequency response characteristics of measurement points, it can be seen that the vibration amplification effect generated by the simultaneous passage mainly reflects in the 40–80 Hz frequency band, while vibration attenuation occurs in other frequency bands. Furthermore, the vibration impact of bus attenuates rapidly as the distance from the centerline increases, and the vertical vibration attenuates more slowly compared to the horizontal vibration.

Conclusion

A field test was carried out in Shenzhen, China, to study the train-induced vibration characteristics in the entry and exit section of a subway station. The test equipment is divided into two groups. One group is arranged in the tunnel to measure the vibration response of rail when the train passes through the straight track and the point of fixed frog; the other group is arranged on the ground at different distances from the subway centerline to collect the acceleration signals under different traffic conditions. The test results are analyzed in the time domain and frequency domain. Relevant data and conclusions can not only guide the design of vibration reduction and isolation schemes for rail transit environmental vibration, but also validate possible numerical prediction models of train-induced vibration. The main conclusions are listed as follows:

(1) The vibration signals measured at the point of fixed frog can clearly distinguish the periodic vibration caused by bogies when the train passes, however, the same phenomenon is not apparent on the straight track, which is due to the fact that the wheel-rail dynamic load excited by a localized rail defect generated sudden dynamic responses. Through statistical analysis of multiple groups of test data, it is found that subway trains in different operating conditions do not have significant different influence on the rail vibration, that is, the vibration levels of the vibration sources are approximately the same.

(2) Compared with the vertical vibration, the horizontal vibration of the ground caused by the passing train is particularly apparent, especially at the position of 20 m and 40 m away from the subway centerline. The amplitude of the horizontal acceleration is significantly greater than the vertical one, and the horizontal vibration is gradually smaller than the latter after 60 m. With the increase of the distance from the centerline, both vertical vibration and horizontal vibration of the ground have a vibration amplification area.

(3) When the near-line train passes the test section, and the far-line train is about to arrive, the vibration amplification mainly occurs within the center frequency of 50–63 Hz compared to when only the near-line train passes; however, it has little effect on the vibration of other frequency bands and even reduces the vibration in some frequency bands.

(4) When the far-line train passes the test section, and the near-line train has just left, the vibration level of each measurement point decreases in various frequency bands to different degrees compared to when only the near-line train passes. The maximum reduction of horizontal acceleration could reach up to 12 dB around 16 Hz.

(5) The simultaneous passage of the near-line train and bus will significantly increase the ground vibration level close to the subway centerline, and the horizontal vibration is more sensitive to the superimposed influence of road traffic. The peak value of the horizontal acceleration at the measuring point 20 m away from the centerline is the largest in the time domain, reaching

2.62×10^{-2} m/s^2, 181.80% higher compared to when only the near-line train passes.

(6) The vertical ground vibration amplification concentrates at 63–80 Hz with an increase of 4.8 dB, and the horizontal vibration amplification occurs at 40–80 Hz with an increase of 6.6 dB. However, the ground vibration levels decrease in other frequency bands. As the distance from the subway centerline increases, the ground vibration level decays rapidly, and the vertical vibration caused by road traffic attenuates more slowly than the horizontal vibration.

CRediT authorship contribution statement

Shuai Qu: Formal analysis, Data curation, Investigation, Methodology, Software, Visualization, Writing - original draft, Writing - review & editing. **Jianjin Yang:** Data curation, Investigation. **Shengyang Zhu:** Funding acquisition, Writing - review & editing, Supervision, Resources, Project administration. **Wanming Zhai:** Funding acquisition, Supervision, Resources, Project administration. **Georges Kouroussis:** Writing - review & editing. **Qinglai Zhang:** Visualization.

Declaration of Competing Interest

The authors declare that they have no known competing financial interests or personal relationships that could have appeared to influence the work reported in this paper.

Acknowledgments

This work was supported by the National Natural Science Foundation of China (No. 11790283, No. 51978587), the Fund from State Key Laboratory of Traction Power (No. 2019TPL-T16) and the Science and Technology Project of Sichuan Province (No. 2021YFH0073), which is gratefully acknowledged by the authors. The authors would like to thank Shenzhen Metro Company and Zhandong Yuan, Xuancheng Yuan, Zhaoling Han, Yun Yang, Zhihao Zhai, Panming Luo, Qiangwen Wei from Train and Track Research Institute for their assistance in the in-situ test and data processing.

References

[1] Amado-Mendes P, Alves Costa P, Godinho LMC, Lopes P. 2.5D MFS-FEM model for the prediction of vibrations due to underground railway traffic. Eng Struct 2015;104:141–54. https://doi.org/10.1016/j.engstruct.2015.09.013.

[2] Auersch L. Simple and fast prediction of train-induced track forces, ground and building vibrations. Railw Eng Sci 2020;28:232–50. https://doi.org/10.1007/s40534-020-00218-7.

[3] Bian XC, Chen YM, Hu T. Numerical simulation of high-speed train induced ground vibrations using 2.5D finite element approach. Sci China, Ser G Physics, Mech Astron 2008;51:632–50. https://doi.org/10.1007/s11433-008-0060-3.

[4] Connolly DP, Galvín P, Olivier B, Romero A, Kouroussis G. A 2.5D time-frequency domain model for railway induced soil-building vibration due to railway defects. Soil Dyn Earthq Eng 2019;120:332–44. https://doi.org/10.1016/j.soildyn.2019.01.030.

[5] Connolly DP, Kouroussis G, Laghrouche O, Ho CL, Forde MC. Benchmarking railway vibrations - Track, vehicle, ground and building effects. Constr Build Mater 2015;92:64–81. https://doi.org/10.1016/j.conbuildmat.2014.07.042.

[6] Connolly DP, Marecki GP, Kouroussis G, Thalassinakis I, Woodward PK. The growth of railway ground vibration problems — A review. Sci Total Environ 2016;568:1276–82. https://doi.org/10.1016/j.scitotenv.2015.09.101.

[7] Crispino M, D'Apuzzo M. Measurement and prediction of traffic-induced vibrations in a heritage building. J Sound Vib 2001;246:319–35. https://doi.org/10.1006/jsvi.2001.3648.

[8] Degrande G, Clouteau D, Othman R, Arnst M, Chebli H, Klein R, et al. A numerical model for ground-borne vibrations from underground railway traffic based on a periodic finite element-boundary element formulation. J Sound Vib 2006;293:645–66. https://doi.org/10.1016/j.jsv.2005.12.023.

[9] Degrande G, Lombaert G. High-speed train induced free field vibrations: in situ measurements and numerical modelling. Proc Int Work Wave 2000;2000:29–41.

[10] Ducarne L, Ainalis D, Kouroussis G. Assessing the ground vibrations produced by a heavy vehicle traversing a traffic obstacle. Sci Total Environ 2018;612:1568–76. https://doi.org/10.1016/j.scitotenv.2017.08.226.

[11] Ge X, Ling L, Yuan X, Wang K. Effect of distributed support of rail pad on vertical vehicle-track interactions. Constr Build Mater 2020;262:120607. https://doi.org/10.1016/j.conbuildmat.2020.120607.

[12] Gupta S, Liu WF, Degrande G, Lombaert G, Liu WN. Prediction of vibrations induced by underground railway traffic in Beijing. J Sound Vib 2008;310:608–30. https://doi.org/10.1016/j.jsv.2007.07.016.

[13] He C, Zhou S, Di H, Shan Y. A 2.5-D coupled FE–BE model for the dynamic interaction between saturated soil and longitudinally invariant structures. Comput Geotech 2017;82:211–22. https://doi.org/10.1016/j.compgeo.2016.10.005.

[14] He C, Zhou S, Guo P, Gong Q. Three-dimensional analytical model for the dynamic interaction of twin tunnels in a homogeneous half-space. Acta Mech 2019;230:1159–79. https://doi.org/10.1007/s00707-018-2330-0.

[15] Hu J, Bian X, Xu W, Thompson D. Investigation into the critical speed of ballastless track. Transp Geotech 2019;18:142–8. https://doi.org/10.1016/j.trgeo.2018.12.004.

[16] Hunaidi O, Guan W, Nicks J. Building vibrations and dynamic pavement loads induced by transit buses. Soil Dyn Earthq Eng 2000;19:435–53. https://doi.org/10.1016/S0267-7261(00)00019-1.

[17] Hung HH, Chen GH, Yang YB. Effect of railway roughness on soil vibrations due to moving trains by 2.5D finite/infinite element approach. Eng Struct 2013;57:254–66. https://doi.org/10.1016/j.engstruct.2013.09.031.

[18] Hussein MFM, François S, Schevenels M, Hunt HEM, Talbot JP, Degrande G. The fictitious force method for efficient calculation of vibration from a tunnel embedded in a multi-layered half-space. J Sound Vib 2014;333:6996–7018. https://doi.org/10.1016/j.jsv.2014.07.020.

[19] Hussein MFM, Hunt HEM. A numerical model for calculating vibration from a railway tunnel embedded in a full-space. J Sound Vib 2007;305:401–31. https://doi.org/10.1016/j.jsv.2007.03.068.

[20] Jones S, Kuo K, Hussein M, Hunt H. Prediction uncertainties and inaccuracies resulting from common assumptions in modelling vibration from underground railways. Proc Inst Mech Eng Part F J Rail Rapid Transit 2012;226:501–12. https://doi.org/10.1177/0954409712441744.

[21] Khan MR, Dasaka SM. Quantification of ground-vibrations generated by high speed trains in ballasted railway tracks. Transp Geotech 2019;20:100245. https://doi.org/10.1016/j.trgeo.2019.100245.

[22] Kouroussis G, Connolly DP, Verlinden O. Railway-induced ground vibrations – a review of vehicle effects. Int J Rail Transp 2014;2:69–110. https://doi.org/10.1080/23248378.2014.897791.

[23] Lombaert G, Degrande G. Experimental validation of a numerical prediction model for free field traffic induced vibrations by in situ experiments. Soil Dyn Earthq Eng 2001;21(6):485–97. https://doi.org/10.1016/S0267-7261(01)00017-3.

[24] Lopes P, Alves Costa P, Calçada R, Cardoso A. Influence of soil stiffness on building vibrations due to railway traffic in tunnels: Numerical study. Comput Geotech 2014;61:277–91. https://doi.org/10.1016/j.compgeo.2014.06.005.

[25] Lu Z, Hu Z, Yao H lin, Liu J. Field evaluation and analysis of road subgrade dynamic responses under heavy duty vehicle. Int J Pavement Eng 2018;19:1077–86. https://doi.org/10.1080/10298436.2016.1240560.

[26] Pyl L, Degrande G, Clouteau D. Validation of a Source-Receiver Model for Road Traffic-Induced Vibrations in Buildings. II: Receiver Model. J Eng Mech 2004;130:1394–406. https://doi.org/10.1061/(asce)0733-9399(2004)130:12(1394).

[27] Ruiz JF, Soares PJ, Alves Costa P, Connolly DP. The effect of tunnel construction on future underground railway vibrations. Soil Dyn Earthq Eng 2019;125. https://doi.org/10.1016/j.soildyn.2019.105756.

[28] Sheng X, Jones CJC, Thompson DJ. Modelling ground vibration from railways using wavenumber finite- and boundary-element methods. Proc R Soc A Math Phys Eng Sci 2005;461:2043–70. https://doi.org/10.1098/rspa.2005.1450.

[29] Sheng X. A review on modelling ground vibrations generated by underground trains. Int J Rail Transp 2019;7:241–61. https://doi.org/10.1080/23248378.2019.1591312.

[30] Shih JY, Thompson DJ, Zervos A. The influence of soil nonlinear properties on the track/ground vibration induced by trains running on soft ground. Transp Geotech 2017;11:1–16. https://doi.org/10.1016/j.trgeo.2017.03.001.

[31] Thompson DJ, Kouroussis G, Ntotsios E. Modelling, simulation and evaluation of ground vibration caused by rail vehicles. Veh Syst Dyn 2019;57:936–83. https://doi.org/10.1080/00423114.2019.1602274.

[32] Watts GR, Krylov VV. Ground-borne vibration generated by vehicles crossing road humps and speed control cushions. Appl Acoust 2000;59:221–36. https://doi.org/10.1016/S0003-682X(99)00026-2.

[33] Watts GR. The generation and propagation of vibration in various soils produced by the dynamic loading of road pavements. J Sound Vib 1992;156:191–206. https://doi.org/10.1016/0022-460X(92)90692-Q.

[34] Xia H, Zhang N, Cao YM. Experimental study of train-induced vibrations of environments and buildings. J Sound Vib 2005;280:1017–29. https://doi.org/10.1016/j.jsv.2004.01.006.

[35] Xu L, Li Z, Zhao Y, Yu Z, Wang K. Modelling of vehicle-track related dynamics: a development of multi-finite-element coupling method and multi-time-step solution method. Veh Syst Dyn 2020. https://doi.org/10.1080/00423114.2020.1847298.

[36] Yang YB, Hsu LC. A review of researches on ground-borne vibrations due to moving trains via underground tunnels. Adv Struct Eng 2006;9:377–92. https://doi.org/10.1260/136943306777641887.

[37] Zhai W, Wei K, Song X, Shao M. Experimental investigation into ground vibrations induced by very high speed trains on a non-ballasted track. Soil Dyn Earthq Eng 2015;72:24–36. https://doi.org/10.1016/j.soildyn.2015.02.002.

[38] Zhang X, Zhou S, He C, Di H, Si J. Experimental investigation on train-induced vibration of the ground railway embankment and under-crossing subway tunnels. Transp Geotech 2021;26:100422. https://doi.org/10.1016/j.trgeo.2020.100422.

[39] Zhu Z, Wang L, Costa PA, Bai Y, Yu Z. An efficient approach for prediction of subway train-induced ground vibrations considering random track unevenness. J Sound Vib 2019;455:359–79. https://doi.org/10.1016/j.jsv.2019.05.031.
[40] Zou C, Wang Y, Moore JA, Sanayei M. Train-induced field vibration measurements of ground and over-track buildings. Sci Total Environ 2017;575:1339–51. https://doi.org/10.1016/j.scitotenv.2016.09.216.
[41] Zou C, Wang Y, Wang P, Guo J. Measurement of ground and nearby building vibration and noise induced by trains in a metro depot. Sci Total Environ 2015;536:761–73. https://doi.org/10.1016/j.scitotenv.2015.07.123.